

AN IMPLEMENTATION OF THE BACK-PROJECTION ALGORITHM ACCORDING TO SANTOSA AND VOGELIUS

Pai Chi Nan

Department of Mechanical Engineering - Polytechnic School of University of São Paulo Av. Prof. Mello de Moraes, 2231 - São Paulo
- SP - 05508-900, Brazil
paichinan@yahoo.com

Julio C. C. Aya

Department of Mechanical Engineering - Polytechnic School of University of São Paulo Av. Prof. Mello de Moraes, 2231 - São Paulo
- SP - 05508-900, Brazil
jccaya@usp.br

Raul Gonzalez Lima

Department of Mechanical Engineering - Polytechnic School of University of São Paulo Av. Prof. Mello de Moraes, 2231 - São Paulo
- SP - 05508-900, Brazil
rauglima@usp.br

Corresponding author: Raul Gonzalez Lima

Abstract. *Electrical Impedance Tomography (EIT) is a technique to estimate the impedance distribution of a domain of interest, for instance, a section of the human body. It uses the boundary electrical potential measurements of the section to estimate the image. One of the early image reconstruction algorithms is called back-projection, duo to Barber and Brown, but there is a lack of articles about it. Santosa and Vogelius proposed an implementation of the Barber-Brown algorithm with interpolation of the boundary data and low-pass filter the image.*

The present work shows an implementation of this improvement with a particular choice of interpolation of the boundary data and an interpretation of the resulting image in terms of resistivity instead of conductivity.

Keywords: *back-projection, Electrical Impedance Tomography*

1. Introduction

The back-projection algorithm, developed by Barber and Brown in 1983, is an efficient algorithm with relative low computer cost [1, 2], and this is the reason for being one of the most well known image reconstruction algorithms for Electrical Impedance Tomography. However, there are few articles describing how is this algorithm. One of these articles was written by Santosa and Vogelius [3]. The vast literature on Backprojection reports its performance or clinical applications.

Backprojection is a two dimensional reconstruction algorithm and, initially, the domain was restricted to be circular. Extensions for non-circular domains were proposed. A three dimensional direct extension of the Barber and Brown Backprojection was not accomplished [4], although some conceptually closely related 3D algorithms were developed [5].

An posterior development, called filtered backprojection [4, 6], improved the spatial resolution and the conductivity resolution pre-processing the electric potential data before the use of the backprojection algorithm. The pre-processing, or filtering procedure, used the first derivative of a finite elements model of the domain under analysis.

The objective of the present work is to describe an implementation the back-projection algorithm according to Santosa and Vogelius, with a particular choice of interpolation of the boundary data and an interpretation of the resulting image in terms of resistivity instead of conductivity using concepts from the calculus of variations.

2. Sheffield's back-projection algorithm

The mathematical representation of the problem is supposed to be [4]

$$\nabla \cdot (\sigma \nabla U) = 0 \text{ in } \Omega \quad (1)$$

$$\sigma \frac{\partial U}{\partial n} = J \text{ on } \partial\Omega \quad (2)$$

where σ is the conductivity profile, U is the electric potential, J is the boundary current density and Ω is the domain of interest.

Taking the first variation of eq. 1 and eq. 2, denoting the first variation of the conductivity by $\delta\sigma$ and the first variation of the electric potential by δU , results,

$$\nabla \cdot (\sigma \nabla \delta U) + \nabla \cdot (\delta \sigma \nabla U) = 0 \text{ in } \Omega \quad (3)$$

$$\sigma \frac{\partial (\delta U)}{\partial n} + \delta \sigma \frac{\partial U}{\partial n} = 0 \text{ on } \partial \Omega \quad (4)$$

With the following hypotheses

1. Ω is the unit two dimensional ball;
2. the conductivity is unitary $\sigma = 1$;
3. $\delta \sigma = 0$ near the dipole

the linearized problem reduces to

$$\nabla^2 \delta U = -\nabla (\delta \sigma) \cdot \nabla U \text{ in } \Omega \quad (5)$$

$$\frac{\partial (\delta U)}{\partial n} = 0 \text{ on } \partial \Omega \quad (6)$$

The linearized inverse problem associated with equations 5 and 6 becomes

Given a variation of electric potential along the boundary, $\delta U|_{\partial \Omega}$, for various choices of dipole positions along the boundary, determine a consistent increment $\delta \sigma$.

To solve this problem, Barber and Brown used a change of variables that mapped the circular domain into a rectangular domain.

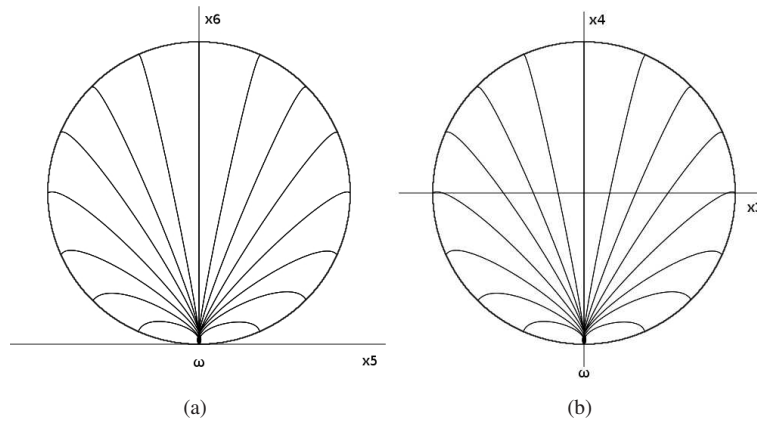


Figure 1. (a) coordinates (x_5, x_6) (b) coordinates (x_3, x_4)

Using the reference frame shown on Fig. 1(a), with ω representing the position of current injecting dipole, which is located between two electrodes, the equation for the voltage equipotential lines is

$$U = \frac{x_5}{x_5^2 + x_6^2} \quad (7)$$

and the equation for the current equipotential lines is

$$V = \frac{x_6}{x_5^2 + x_6^2} \quad (8)$$

With a translation on the reference frame, see Fig. 1(b), equations 7 and 8 become

$$U = \frac{x_3}{x_3^2 + (x_4 + 1)^2} \quad (9)$$

$$V = \frac{(x_4 + 1)}{x_3^2 + (x_4 + 1)^2} \quad (10)$$

With the equations 9 and 10, the domain Ω can be mapped to the upper half plane P defined by the rectangular region where $V > 1/2$. The problem represented by equations 5 and 6 simplifies, using the new coordinates (U, V) , to

$$\nabla^2 \delta U = -\frac{\partial(\delta\sigma)}{\partial U} \text{ in } P \quad (11)$$

$$\frac{\partial(\delta U)}{\partial V} = 0 \text{ on } \partial P = \{V > \frac{1}{2}\} \quad (12)$$

Barber and Brown suggest that the average

$$\delta\sigma = \frac{1}{m} \sum_{j=1}^m W(s, \omega_j) |_{s=U(s, \omega_j)} (2V(x, \omega_j) - 1) \quad (13)$$

as the discrete solution for $\delta\sigma$, where m is the number of the electrodes, W is the voltage measurement on the boundary, ω represent the position of the electrode and V is the current intensity function. Santosa and Vogelius have shown that eq. 13 is a simplification of the one consistent with the Radon Transform [?].

Since the voltage measurement is affected by the resistivity/conductivity of the whole of the body, Barber and Brown suggest the use of a normalized voltage measurement to obtain a normalized conductivity.

The Sheffield back-projection algorithm assumes that the region between two adjacent potential lines has the same voltage measurement. Rotating the position of the current injection dipole, it obtains m sets of voltage measurements. These sets of electric potential measurements, , previously normalized, adjusted by the corresponding weight, which is $2V - 1$, is the desired normalized conductivity.

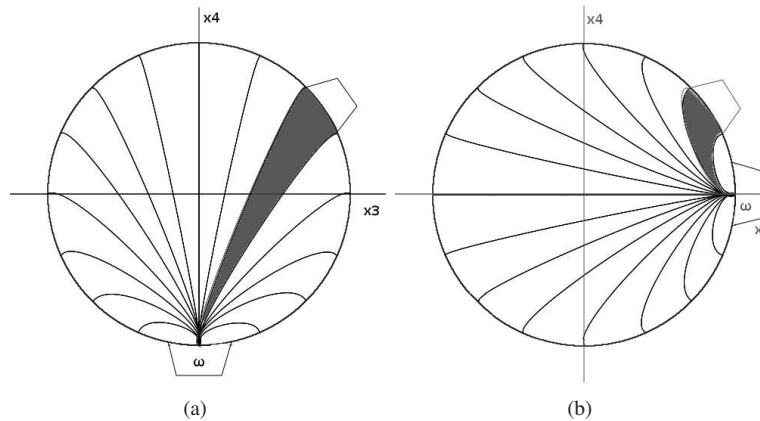


Figure 2. Different positions of current injection electrode

3. Improvement of back-projection by Santosa and Vogelius

Santosa and Vogelius suggested that instead of using the region between two equipotential lines, the algorithm should find the corresponding electric potential measurement for a certain point inside the domain, according to the equipotential lines. Since there is a limited number of electric potential measurements on the boundary, they suggest a linear interpolation to find these measurements.

From the orientation and position of the electrode shown on Fig. 1(b), it is possible to find the point on the boundary of the domain with the same electric potential measurement of the point desired by equations 14 and 15

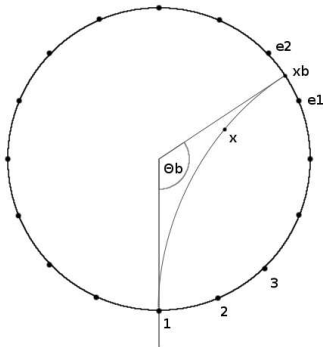


Figure 3. The electric potential measurement of certain point x

$$x_{b3} = \frac{4U}{4U^2 + 1} \quad (14)$$

$$x_{b4} = \frac{2}{4U^2 + 1} - 1 \quad (15)$$

Using the equations 14 and 15, and linear interpolation between electrodes $e1$ and $e2$, we obtain the electric potential measurements, which are differential measurements, of all the pixels inside the domain. Rotating the current injection pattern, other sets of measurements can be obtained. And the normalized conductivity distribution is

$$\frac{\delta\sigma_i}{\sigma_i} = -\frac{1}{m} \sum_{j=1}^m \frac{\delta U_j}{U_j} (2V_{i,j} - 1) \quad (16)$$

where i represent the pixels, j represent a pair of electrodes, $\delta\sigma_i$ is the perturbed conductivity, σ_i is the conductivity of reference, m is the total number of pair of electrodes, δU_j is the perturbed electric potential, U_j is the electric potential of reference, and $V_{i,j}$ is the equipotential line corresponding to the current passing through the desired point.

The equations 14 and 15 are for dipole at position 1, or $-\pi/2$. With the rotation of the current injecting electrodes, it is necessary to change coordinates according to

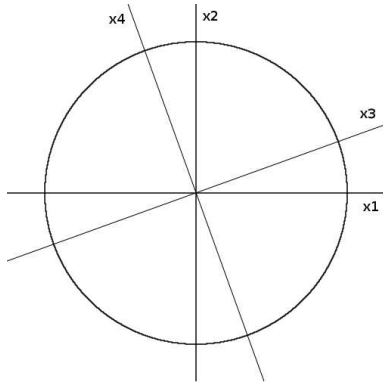


Figure 4. Relation between $(x3,x4)$ and $(x1,x2)$

$$x_3 = x_1 * \cos\theta + x_2 * \sin\theta \quad (17)$$

$$x_4 = -x_1 * \sin\theta + x_2 * \cos\theta \quad (18)$$

4. Conductivity X Resistivity

The two methods described before give images of distribution of conductivity. For medical interpretation, images given in term of distribution of resistivity are better. Using concepts of calculus of variations, the relation of both images is straightforward

$$\frac{\delta\sigma}{\sigma} = \frac{\delta\left(\frac{1}{\rho}\right)}{\frac{1}{\rho}} = \frac{-\frac{\delta\rho}{\rho^2}}{\frac{1}{\rho}} = -\frac{\delta\rho}{\rho} \quad (19)$$

Therefore, equation 19 is rewritten as

$$\frac{\delta\rho}{\rho} = \frac{1}{m} \sum_{j=1}^m \frac{\delta U}{U} (2V - 1) \quad (20)$$

5. Results

Five images resulting from experimental data are presented. All of them were obtained through the back-projection algorithm as described by Santosa and Vogelius (1990), with the interpretation in terms of resistivity. These images were obtained using a cylindrical acrylic object placed at the center of an experimental cylindrical container, then 30 mm apart from the center, then 60 mm apart from the center, then 90 mm apart from the center and, finally, 120 mm apart from the center of the container, as shown on Fig. 5.

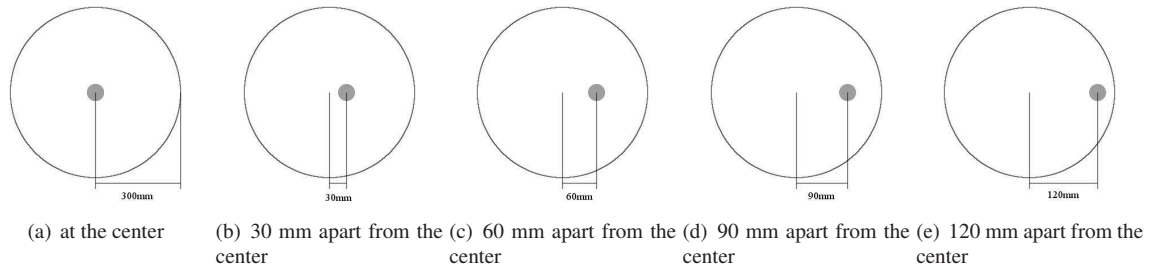


Figure 5. An acrylic object placed inside an cylindrical container with 300mm of diameter

The cylindrical object has 30 mm of diameter, the experimental cylindrical container has 300 mm of diameter and the container was filled with 20 mm of 0.9% saline solution. On the border of the container there are 30 electrodes placed at equal distances. The electrodes were used to measure the electric potential variation due to a disturbance caused by the presence of the acrylic object and the injection of current through an adjacent of these electrodes. These electric potential measurements have accuracy of 2.5 mV and the results are shown in Fig. 6.

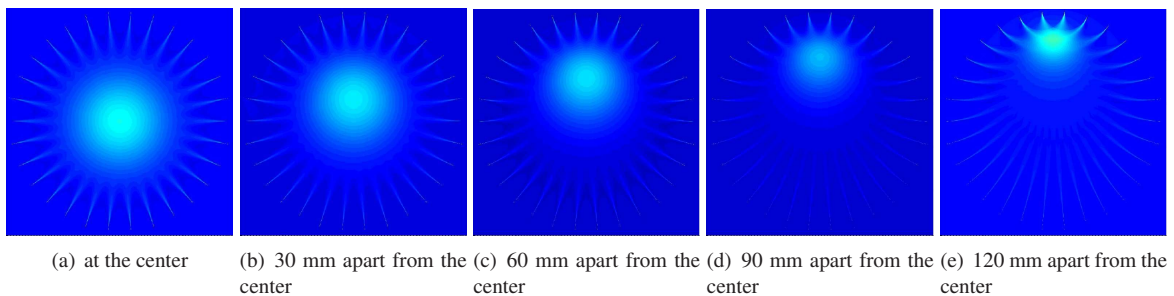


Figure 6. Images estimated

The results show clearly the non-uniform sensitivity of the algorithm. The increasing blurring of the object when the object is closer to the center of the domain is one of the performance problems of this method. The filtered Backprojection has better performance in terms of resolution and sensitivity matrix based algorithms have, to some extent, more uniform sensitivity and spatial resolution [7, 8, 9].

6. Final Comments

The back-projection algorithm was implemented and described. The algorithm was tested and some of its performance characteristics were confirmed. The algorithm has non-uniform sensitivity, as can be seen on the resulting images. At the center of the container, the acrylic object is seen blurred, while at the boundary the image is better defined. The mapping from conductivity distribution into resistivity distribution is simply a multiplication by minus one, when the images are characterized by small deviations from a uniformly distributed value of conductivity or resistivity.

7. Acknowledgments

Financial Supports by The State of São Paulo Research Foundation, process 01/05303-4 is gratefully acknowledged.

8. References

- Yorkey, T.J. and Webster, J.G., 1986, "Comparison Of Impedance Tomographic Reconstruction Algorithms", *Clinical Physics and Physiological Measurement*, vol.8 supp A, pp.55 - 62.
- Brown, B.H., Barber D.C. and Seagar A.D., 1988, "Applied potential tomography: possible clinical applications", *Clinical Physics and Physiological Measurement*, vol. 6 num. 2, pp.109 - 121.

- Santosa, F. and Vogelius, M., 1990, "Backprojection algorithm for electrical impedance imaging", *SIAM Journal on Applied Mathematics*, vol.50, No. 1, pp.216 - 243.
- Metheral, P., 1998, "Three Dimensional Electrical Impedance Tomography of the Human Thorax", PhD thesis, University of Sheffield
- Kotre, C. J. 1994, EIT Image Reconstruction using sensitivity weighted filtered backprojection, *Physiological Measurements*, vol. 15, pp. A125-A136.
- Avis, N.J. and Barber, D.C., 1995, "Incorporating a priori information into the Sheffield filtered backprojection algorithm", *Physiological Measurements*, vol.16 supp A, pp.111-122.
- Adler, A. and R. Guardo 1996, "Electrical Impedance Tomography: Regularized Imaging and Contrast Detection", *IEEE Trans. on Medical Imaging*, vol. 15, no. 2, April, 1996, pp. 170-179. *Clinical Physics and Physiological Measurement*, vol.8 supp A, pp.55 - 62.
- Aya, J.C.C., de Moura, F.S., Pai, C.N., Bevilacqua, J.C., Lima, R.G., 2005, "Back-Projection Resolution Improvement Through Measurement Interpolation Using The Finite Element Method", *Proceedings of TMSi 2005*.
- Wedberg, T.C., Stamnes, J.J. and Singer, W., 1995, "Comparison of the filtered backprojection and the filtered backprojection algorithms for quantitative tomography", *Applied Optics*, vol.34, num.38, pp.65-75.

9. Responsibility notice

The authors are the only responsible for the printed material included in this paper